

Spatial comparison of total vs. active bacterial populations by coupling genetic fingerprinting and clone library analyses in the NW Mediterranean Sea

Arturo Rodríguez-Blanco^{1,2}, Jean-François Ghiglione^{1,2}, Philippe Catala^{1,2}, Emilio O. Casamayor³ & Philippe Lebaron^{1,2}

¹UPMC Univ Paris 06, UMR 7621, Laboratoire ARAGO, Banyuls-sur-Mer, France; ²CNRS, UMR 7621, Laboratoire d'Océanographie Biologique de Banyuls, Banyuls-sur-Mer, France; and ³Limnology Group-Department of Continental Ecology, Centre d'Estudis Avançats de Blanes (CEAB)-CSIC, Carrer d'Accés a la Cala Sant Francesc, Girona, Spain

Correspondence: Jean-François Ghiglione, CNRS, UPMC Univ Paris 06, UMR 7621, Laboratoire d'Océanographie Biologique de Banyuls, Avenue Fontaulé, BP44, F-66650 Banyuls-sur-Mer, France. Tel.: +33 4 68 88 73 16; fax: +33 4 68 88 73 98; e-mail: ghiglione@obs-banyuls.fr

Received 22 February 2008; revised 25 June 2008; accepted 30 July 2008.
First published online 23 October 2008.

DOI:10.1111/j.1574-6941.2008.00591.x

Editor: Patricia Sobczyk

Keywords

CE-SSCP fingerprinting; 16S rRNA; spatial distribution; bacterial diversity and activity *Prochlorococcus*; SAR11; *Gammaproteobacteria*.

Abstract

Spatial distributions of both total (i.e. 16S rDNA-based fingerprints) and active (i.e. 16S rRNA-based fingerprints) bacterial populations, together with total bacterial activity measured by ³H-leucine incorporation, were studied along a 98 km transect in the NW Mediterranean Sea. Capillary electrophoresis-single strand conformation polymorphism (CE-SSCP) fingerprinting was coupled to a clone library, allowing CE-SSCP peaks identification and the monitoring of the spatial variation of bacterial phylotypes. Up to 80% of the community peaks matched those obtained from clone library sequences, accounting for 86.7% of the total fingerprinting area. A good agreement was found between the relative abundance of *Prochlorococcus* in the CE-SSCP fingerprints and flow cytometry counts ($r^2 = 0.66$, $P < 0.05$). The largest differences between total and active bacterial populations distribution were found at depths with higher bacterial activity (i.e. surface and deep chlorophyll maximum, DCM). SAR11 at the surface and *Gammaproteobacteria* at the DCM were the most abundant groups on the 16S rDNA-based fingerprints. However, their ratio of relative importance between rRNA:rDNA was < 1 in most cases. Conversely, ratios observed for *Prochlorococcus*, were consistently > 1 both at the surface and at the DCM. These results emphasize the need for combining rDNA- and rRNA-based analyses to better understand the functional role of individual bacterial populations *in situ*.

Introduction

Bacteria are recognized as having a key role in marine biogeochemical cycles, especially in oligotrophic waters where efficient recycling processes are crucial (Cho & Azam, 1990). Linking horizontal and vertical distributions of bacterial diversity with both metabolic activities and physicochemical gradients is necessary for fully understanding the role of bacteria in the microbial food web (Azam *et al.*, 1983; Pernthaler & Amann, 2005). Studies focusing on horizontal distributions suggested different trends in bacterioplankton community structure. Slight differences were found between bacterioplankton communities in surface waters from stations located a few kilometers apart near Anvers Island, Antarctica (Murray *et al.*, 1998), or even

among heterotrophic bacterial assemblages along 1500 km in the Arabian Sea (Riemann *et al.*, 1999). Other studies showed significant differences between bacterial communities from coastal and offshore stations in the NW Mediterranean Sea (Schauer *et al.*, 2000; Ghiglione *et al.*, 2005). Along the vertical axis, general agreement exists that changes in bacterial assemblages are more perceptible. Bacterial community structure from the euphotic zone, and especially from the deep chlorophyll maximum (DCM) have been described systematically as different from those inhabiting deeper waters (e.g. Lee & Fuhrman, 1991; Acinas *et al.*, 1997; Ghiglione *et al.*, 2007). These differences have been related to the vertical changes in physicochemical conditions.

All these studies were focused on 16S rDNA-based distributions, which do not provide clues on the level of

activity of each detected bacterial population. Bacterial growth rate has been shown to correlate with cellular rRNA content (DeLong *et al.*, 1989; Poulsen *et al.*, 1993); therefore, information on cellular activity may be obtained by tracking reverse-transcribed 16S rRNA (e.g. Casamayor *et al.*, 2001). Even though the abundance of bacteria in the sea is high, only a small fraction is considered to be metabolically active (Sherr *et al.*, 1999; Del Giorgio & Bouvier, 2002). Thus, the community picture gained by looking either at the 16S rDNA or at the 16S rRNA may differ significantly. Only a handful of studies in the literature have combined rDNA- and rRNA-based surveys for the simultaneous description of total (understood as those targeted bacteria above the detection limit of the PCR method) and active (i.e. from the former pool those with a higher rRNA content) bacterioplankton populations, respectively (Moeseneder *et al.*, 2001, 2005; Troussellier *et al.*, 2002; Winter *et al.*, 2004). These studies highlighted these differences, thus reinforcing the idea that the characterization based only on the abundance of rDNA does not offer a consistent view of the most active components of the bacterial assemblage.

Within this framework, the goal of the present study was to follow vertical variations of both the total and the active bacterial populations along a 98 km transect in offshore NW Mediterranean Sea waters. Capillary electrophoresis-single strand conformation polymorphism (CE-SSCP) genetic fingerprints based on both 16S rDNA and 16S rRNA were directly compared. CE-SSCP analyses coupled to a 16S rDNA-based clone library built from a representative sample were used for CE-SSCP peaks' identification and the monitoring of specific qualitative and quantitative changes of bacterial populations along the transect.

Materials and methods

Study site and general sampling methods

The sampling cruise was carried out in the Northwestern Mediterranean Sea on the oceanographic R/V 'Tethys' in July 2004. Water samples from three stations along a 98 km transect (Fig. 1a), i.e. Microbial Observatoire Laboratoire

Arago (for MOLA, 42°26'N–03°32'E, located 36 km apart from Banyuls-sur-mer), S1 (42°20'N–04°00'E, 40 km apart from MOLA) and S2 (42°07'N–04°37'E, 58 km apart from S1) were collected. Four depths were sampled for each station with 10-L Niskin bottles attached to a Sea-Bird conductivity–temperature–depth CTD profiler, according to the *in situ* measured water mass stratification and chlorophyll fluorescence profiles as follows: 5 m, DCM (between 60 and 80 m depth depending on the station), 20 m below the DCM and 150 m depth. Chlorophyll *a* (Chl *a*) concentrations were obtained from 50- to 200-mL water samples (in duplicate) filtered through 47-mm GF/F filters (Whatman, Kent, UK) and frozen in liquid nitrogen until analysis. Pigments were extracted in 90% acetone for 12 h at 4 °C in the dark, and Chl *a* concentrations were determined using a Perkin-Elmer MPF 66 spectrofluorometer (Neveux & Panouse, 1987).

Picophytoplankton and bacterioplankton abundances

Triplicate seawater samples (3 mL) were fixed with 2% formaldehyde for at least 1 h at 4 °C in the dark before quick-freezing in liquid nitrogen and storage at –80 °C. The samples were later thawed at room temperature, and analyzed using a flow cytometer (FACScan, Becton Dickinson, San Jose, CA) equipped with a 488 nm, 15 mW Argon laser for analyses. Fluorescent beads (1.0 µm; Polysciences Inc., Warrington, PA) were added to each sample to normalize the forward and right angle light scatter (FSC and SSC) and green (515–545 nm), orange (564–606 nm) and red (> 650 nm) fluorescence signals, respectively. For picophytoplankton analysis, 1 mL subsamples were run at a high speed (*c.* 50 µL min⁻¹) and counted for 5 min, using red fluorescence as the threshold parameter. The *Prochlorococcus* sp. abundance was counted on a red fluorescence vs. SSC cytogram, as described by Joux *et al.* (2005). For bacterioplankton analysis, subsamples of 1 mL were stained with a nucleic acid dye [SYBR Green II; final concentration 0.05% (v/v) of the commercial solution; Molecular Probes Inc., OR] for at least 15 min at 20 °C in the dark and analyzed for

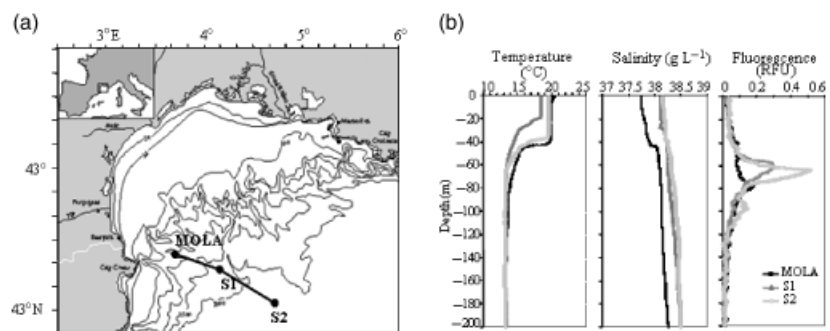


Fig. 1. Study site location (a), hydrological and fluorescence (b) parameters measured during a 98 km linear transect along the offshore stations MOLA S1 and S2 in the NW Mediterranean Sea.

1 min three consecutive times. Bacteria were counted using the plot of green fluorescence vs. SSC and the green fluorescence was used as the threshold parameter.

Bacterial production (BP)

BP was measured by ^3H -leucine incorporation (Kirchman, 1993) as modified from Smith & Azam (1992). Water samples (2.5 mL in triplicate) were added to a sterile polystyrene snap cap tube (5 mL), containing 8 nM ^3H -leucine (specific activity 117 Ci mmol $^{-1}$, Perkin-Elmer, Wellesley, MA) and 32 nM of unlabelled leucine. One killed control was prepared for each assay by addition of 250 μL of 50% trichloroacetic acid (TCA), 15 min before the leucine addition. Tubes were incubated in the dark at the *in situ* temperature for 1 h. The reaction was stopped by transferring replicate 1 mL samples from each tube into microcentrifuge tubes containing 100 μL of 50% TCA. Samples were stored for at least 1 h at 4 °C and then centrifuged for 15 min at 12 000 g. The precipitate was rinsed once with 5% TCA and once with 70% ethanol, resuspended in 1 mL of liquid scintillation cocktail (FilterCount, Perkin-Elmer) and Radioactivity uptake was determined on a liquid scintillation counter (LS 5000CE Beckman). Leucine incorporation rates were converted into carbon production using a conversion factor of 1.55 kg C produced by mole of leucine incorporated (Kirchman, 1993). The analytical accuracy of measurements yielded a coefficient of variation < 4%.

DNA extraction and purification

Two liters of each water sample were prefiltered with a 3- μm pore-size filter (47 mm, Polycarbonate, Nuclepore[®], Whatman, Kent, UK) and then filtered throughout a 0.22- μm pore-size filter (47 mm, Polycarbonate, Nuclepore[®]) before being stored at -80 °C until analysis. DNA was extracted in lysis buffer (50 mM Trizma base, 40 mM EDTA and 0.75 M sucrose) by first adding a freshly prepared lysozyme solution (final concentration 1 mg mL $^{-1}$) and incubating at 37 °C for 45 min. Sodium dodecyl sulfate (final concentration 1%) and a proteinase K solution (final concentration 0.2 mg mL $^{-1}$) were then added and tubes were incubated at 50 °C for 1 h. A 600 μL volume of the resulting cellular lysate was treated with 10 μL of a 100 mg mL $^{-1}$ RNase A solution (Qiagen, Hilden, Germany) before DNA extraction was carried out using the DNeasy Tissue kit (Qiagen), as described by the manufacturer's instructions.

RNA extraction and cDNA synthesis

Samples for RNA analysis were processed in parallel to the DNA extractions. The remaining 400 μL of the lysate was treated with DNase I for RNA extraction using an SV Total RNA Isolation kit (Promega, Madison, WI). The efficiency

of DNA digestion was checked using direct PCR amplification (conditions as reported below), being those reactions that yielded no PCR product used for cDNA synthesis. RNA was reverse transcribed (RT) into single-strand cDNA using Moloney murine leukemia virus (MMLV) reverse transcriptase (Promega), according to the manufacturer's instructions. PCR amplification of cDNA was carried out as for DNA.

PCR-CE-SSCP fingerprinting

The highly variable V3 region (*Escherichia coli* 16S rRNA gene positions 329–533, Brosius *et al.*, 1981) of the 16S rRNA gene was amplified for both DNA and cDNA extracts. Bacterial universal primers set w49 forward (5'-ACG GTC CAG ACT CCT ACG GG-3'; Delbès *et al.*, 2001) and w34 reverse (5'-TTA CCG CGG CTG CTG GCA C-3'; Lee *et al.*, 1996) were used. The reverse primer was fluorescently labelled with phosphoramidite (TET, Applied Biosystems, Applied Biosystems, Norwalk, CT) at the 5'-end position. Primers have been checked using the Probe Match tool provided by the Ribosomal Database Project containing 371 022 bacterial sequences for the range 329–533 of *E. coli* positions (Brosius *et al.*, 1981). Primer w49 forward matched 348 645 of total available 371 022 sequences while primer w34 reverse matched 358 635 of 371 022 total available sequences. Both of these results were obtained when the number of mismatches permitted was two. PCR amplification of 50- μL reactions containing template, primers (final concentration 0.25 μM), dNTPs (Eurogentec, Seraing, Belgium, final concentration 0.6 mM), *Pfu* DNA polymerase (1 U, Promega) and *Pfu* reaction buffer were processed in a Robocycler thermocycler (Stratagene, Agilent Technologies, Santa Clara, CA). The PCR steps were: initial denaturation at 94 °C for 1 min, followed by 25 cycles of denaturation at 94 °C for 1 min, annealing at 61 °C for 15 s and extending at 72 °C for 30 s, with a final 10-min extension at 72 °C. Size (*c.* 200 bp length) and concentration of the PCR products were determined using agarose gel electrophoresis (2%) with a DNA size standard (Low DNA Mass Ladder, GIBCO, Invitrogen Corp., Carlsbad, CA).

Dilutions in nuclease-free sterile water were made to obtain 10 ng μL^{-1} of PCR product. One microliter of the diluted solution was mixed with 18.9 μL of formamide (Applied Biosystems) and 0.1 μL of the internal size standard Gene-Scan-400 Rox (Applied Biosystems, Applied Biosystems), denatured at 94 °C for 5 min and immediately cooled on ice for 5 min and then electrokinetically injected (5 s, 12 kV) into a capillary tube (47 cm \times 50 μm) filled with 5.6% of Gene Scan polymer in a ABI PRISM 310 Genetic analyzer (Applied Biosystems). Electrophoresis was carried out at 15 kV for 30 min per sample at 30 °C and data were collected with ABI PRISM 310 collection software (Applied Biosystems).

TET-labelled fragments were detected by a laser with a virtual C filter (detection wavelengths 532, 537 and 584 nm). Data were collected with ABI PRISM 310 collection software (Applied Biosystems). In order to normalize the different runs, all electropherograms were calibrated by fixing the positions of peaks produced by the added internal size standard GeneScan-400 Rox (Applied Biosystems) and then using a second-order least-square curve (i.e. linear regression) to provide the best interline comparison (GENESCAN ANALYSIS software, Applied Biosystems). Almost no variation among replicate samples had been shown previously for this technique (Ghiglione *et al.*, 2005), thus allowing a reliable comparative analysis among CE-SSCP profiles. Unweighted-pair-group method with arithmetic averages (UPGMA) Euclidean distance dendrograms were constructed with the SAFUM software (Zemb *et al.*, 2007) from a matrix taking into account the presence or absence of individual peaks (qualitative analysis) and the relative contribution of each peak (in percentage) to the total intensity of the whole fingerprint (quantitative analysis). Peak detection was achieved by computing the first derivative of a polynomial curve fitted to the data within a window that was centered on each data point (GENESCAN ANALYSIS software, Applied Biosystems). Because many overlapping peaks were present in our profiles, we used a high polynomial degree value of 19 in order to increase peak detection sensitivity.

Clone library construction

DNA obtained from samples collected at 80 m depth from the MOLA station served to amplify the complete 16S rRNA gene using primers SAdir forward (5'-AGAGTTTGATCATGGCTCAG-3'; *E. coli* 16S rRNA gene positions 8–27) and S17 reverse (5'-GTTACCTTGTTACGACTT-3'; *E. coli* 16S rRNA gene positions 1491–1508) (numbering after Brosius *et al.*, 1981). Reaction mixtures of 50 µL contained DNA template, primers (final concentration 1 µM), dNTPs (final concentration 0.6 mM) and 1 U of Super Taq polymerase (HT Biotechnology, Cambridge, UK) and specific buffer. The PCR program was as follows: 94 °C for 3 min, followed by 30 cycles of 94 °C for 1 min, 50 °C for 1 min and 72 °C for 2 min. The final elongation step was 10 min at 72 °C. The 16S rDNA products were analyzed using electrophoresis in 1% agarose gels and cloned using the TOPO TA cloning kit for sequencing (Invitrogen) according to the manufacturer's protocol. The inserts were PCR amplified from randomly selected colonies using M13 forward and M13 reverse primers. The resulting library of M13 PCR products was composed of 154 clones from which 94 were sequenced (Genome Express, France) based on different restriction fragment length polymorphism (RFLP) genetic profiles using Hin6 and RsaI restriction enzymes.

Useful sequences were obtained from 80 clones that were manually corrected using CHROMAS software (Technelysium) and checked for chimera presence using the ExpASy proteomics server facilities. Phylogenetic identification was based on the closest relative after a BLAST search (<http://www.ncbi.nlm.nih.gov/blast>) and on the phylogenetic tree topography after sizing down to a homogeneous 591-bp sequence length (*E. coli* 16S rRNA gene positions 246–837) using BIOEDIT v5.0.9 (North Carolina State University) and CLUSTALX (Thompson *et al.*, 1997). Sequences were deposited in Genbank under accession numbers AM748176–AM748255. Rarefaction curves were obtained using the DOTUR software (Schloss & Handelsman, 2005; <http://www.plantpath.wisc.edu/fac/joh/dotur.html>) using as an input file a distance matrix generated by the PHYLIP software package (<http://evolution.genetics.washington.edu/phylip.html>).

Identification of community CE-SSCP peaks by single clone assignments

The V3 region of the 16S rDNA was also amplified for each of the 80 sequenced clones using the same PCR-CE-SSCP fingerprinting procedure as described above. Single-peak profiles of all clones were aligned to the profile obtained from the whole community assemblage of the same sample (i.e. 80 m depth at MOLA station) by using the GeneScan-400 Rox internal standard. The phylogenetic identity of a given community peak was provided by the phylogenetic affiliation of the clone showing the same electrophoretic migration. If several clones matched the same community peak, the most frequently recovered phylotype among the clones was defined as being representative.

Results

Sampling sites' characterization

Locations of the three stations MOLA, S1 and S2 and the hydrological and fluorescence parameters measured in July 2004 are shown in Fig. 1. Data showed a strong thermal stratification for all stations. At the MOLA and S2 stations, a temperature gradient was observed, ranging from 20 °C at the surface, decreasing rapidly to 15 °C at 40 m depth and remaining fairly constant below the thermocline (13.5 ± 0.3 °C). The same trend was observed for the S1 station, with a broader thermocline between 20 and 40 m. Salinity was slightly higher at S1 and S2 stations (38.3 ± 0.2 g NaCl L⁻¹) compared with MOLA (38.0 ± 0.2 g NaCl L⁻¹), especially in the first 40 m depth ($\delta_{\text{salinity S1, S2 - MOLA}} = 0.4$ g NaCl L⁻¹). The fluorescence maximum differed in depth and intensity among the three stations. A sharp fluorescence peak was observed at MOLA 80 m corresponding to a DCM of $0.54 \mu\text{g L}^{-1}$ Chl *a*. Thicker and more intense fluorescence peaks were found for the other

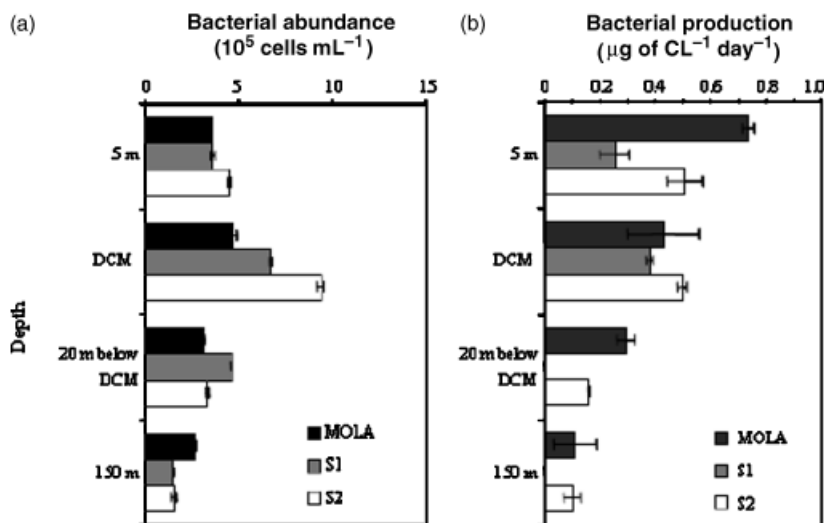


Fig. 2. Vertical changes of BA (a) and BP (b) measured at the MOLA, S1 and S2 stations.

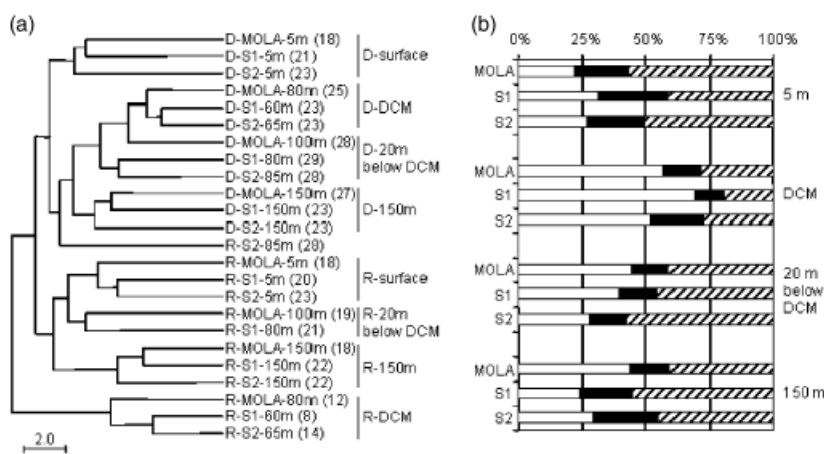


Fig. 3. Community structure of samples from stations MOLA, S1 and S2. (a) UPGMA Euclidean distance dendrogram generated from 16S rDNA (D) and 16S rRNA (R) CE-SSCP profiles. Scale bar indicates the Euclidean distance. (b) Percentage among each pair of rDNA- and RNA-based profiles, of ribotypes found on both rDNA and rRNA profiles (hatched), on 16S rDNA-based profiles only (white), and on 16S rRNA-based profiles only (black).

two stations (ranging in depth between 55 and 80 m) with a DCM of $1.17 \mu\text{g L}^{-1}$ Chl *a* at 60 m for station S1 and $1.81 \mu\text{g L}^{-1}$ Chl *a* at 65 m for station S2.

Bacterial abundance (BA) and BP

The highest values of BA (i.e. heterotrophic prokaryotes) were found at the DCM for all stations (Fig. 2a), i.e., MOLA (4.2×10^5 cells mL^{-1}), S1 (6.7×10^5 cells mL^{-1}) and S2 (9.3×10^5 cells mL^{-1}). The increase of BA from the surface to the DCM was more marked for S1 and S2 than for MOLA ($\delta\text{BA}_{\text{surface-DCM}}$ of 3.1×10^5 , 5.1×10^5 and 0.3×10^5 cells mL^{-1} , respectively). In all cases, BA decreased with depth, reaching about 2.0×10^5 cells mL^{-1} at 150 m.

Overall BP presented higher values at the surface (average value for the three stations of $0.50 \mu\text{g CL}^{-1} \text{day}^{-1}$, $\text{SD} = 0.24$) and DCM depth ($0.44 \mu\text{g CL}^{-1} \text{day}^{-1}$, $\text{SD} = 0.06$) than in

deeper waters (the averaged value 20 m below DCM was $0.15 \mu\text{g CL}^{-1} \text{day}^{-1}$, $\text{SD} = 0.15$, whereas at 150 m it was $0.07 \mu\text{g CL}^{-1} \text{day}^{-1}$, $\text{SD} = 0.06$, Fig. 2b).

Qualitative and quantitative comparative analysis of CE-SSCP fingerprints based on 16S rDNA and 16S rRNA

The UPGMA dendrogram based on both CE-SSCP peaks presence/absence and relative abundance showed that rDNA and rRNA-based fingerprints presented low similarity because they formed separate clusters (except for the rRNA-based profile from 20 m below the DCM at S2 station; Fig. 3a). However, samples from the same depth (i.e. surface, DCM, 20 m below the DCM and 150 m) collected from the three stations presented high similarity because they clustered together in both rDNA and rRNA-based branches

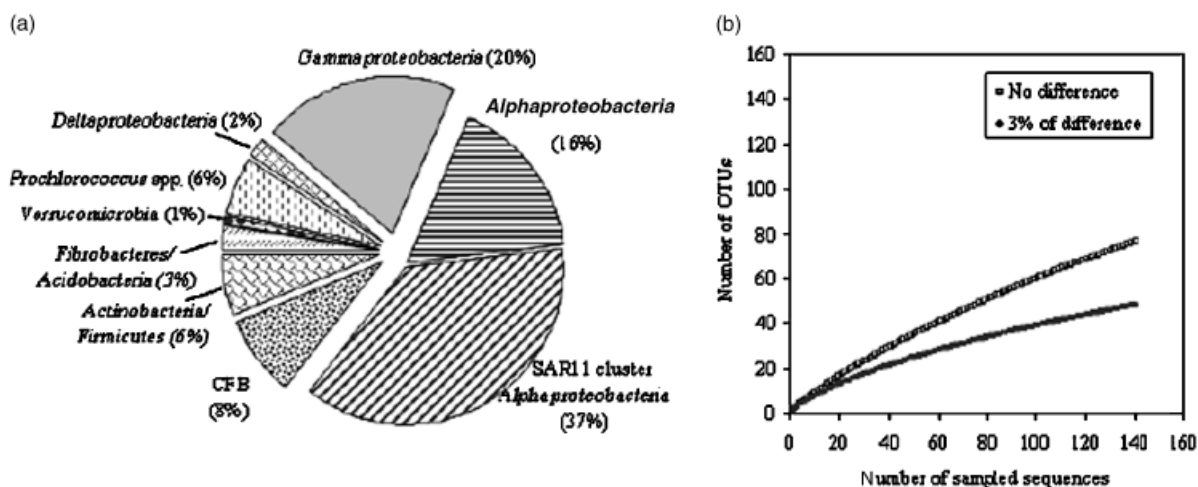


Fig. 4. (a) Phylogenetic composition of the clone library based on 16S rDNA from a sample collected at the DCM depth in the MOLA station. Segments of the pie charts represent the relative abundance of the different bacterial groups (values indicated in brackets), considering the total number of clones (154) in the RFLP screening. (b) Rarefaction curves built from a distance matrix based on DNA sequences.

(except for the rRNA-based profile from 20 m below the DCM at S2 station and the rDNA-based profile from 20 m below the DCM at MOLA station; Fig. 3a).

The largest variation among bacteria from different depths was observed at the surface for 16S rDNA-based profiles and at DCM for 16S rRNA-based profiles with respect to other depths (Fig. 3a).

The highest number of peaks was found for profiles from 20 m below DCM on rDNA- (28–29 peaks) and rRNA-based (19–24) fingerprints (Fig. 3a). The lowest number of peaks was found at the surface (18–23 peaks) for rDNA-based profiles whereas it was found at DCM for rRNA-based profiles (8–14 peaks, Fig. 3a).

The percentage of shared peaks among pairs of rDNA- and rRNA-based profiles from each sample revealed that ribotypes were mostly shared at the surface, 20 m below DCM and at 150 m. Interestingly, at the DCM most of the ribotypes were only detected in the rDNA-derived fingerprints (Fig. 3b).

Analysis of the clone library and identification of CE-SSCP peaks

Relative coverages of the different bacterial phylotypes found at the DCM (80 m) in MOLA station are shown in Fig. 4a. *Proteobacteria*-related clone sequences accounted for 75% of the total and within this group the Alpha class reached more than a half of the total sequences (53%), representing the SAR11 cluster 37% and the *Roseobacter* clade 2%. *Gammaproteobacteria* represented 20% of the total (from which 5% belonged to SAR86 cluster) and *Deltaproteobacteria* only 2% of the sequences. *Bacteroidetes* (formerly CFB phylum) accounted for 8% of the clone

library, *Prochlorococcus* up to 6% and *Actinobacterial/Firmicutes* 6%. Other minor groups were identified as *Fibrobacteres/Acidobacteria* phyla (3%) and *Verrucomicrobia* phylum (1%). Rarefaction curves constructed from a distance matrix based on DNA sequences showed that the tendency of the curve, for a difference lower than 3%, tended to stabilize with the number of sampled sequences (Fig. 4b).

16S rDNA-based CE-SSCP profiles were obtained from each clone and aligned to a 16S rDNA-based community profile obtained from the same sample (i.e. DCM depth at MOLA station, Fig. 5). Twenty out of 25 community peaks (80%) were matched by clone-based peaks. This coverage represented 86.7% of the total fingerprinting area in the community profile. Eighty-five per cent of community peaks (i.e. 17 out of 20) presented a most frequently matching phylotype allowing assignment with different levels of confidence (see right column in Fig. 5), and 45% of them (nine out of 20) were unequivocally assigned to a single phylotype. For three out of the 20 peaks (peaks 3, 14 and 22, marked as nondetermined in Fig. 5), several equally abundant clones from distantly related groups comigrated in the same position; therefore, they could not be identified.

Clones belonging to a single phylotype happened to match different community peaks, this was occasionally related to differences regarding the V3 region of the 16S rDNA. Among SAR11 sequences matching peaks 10th, 11th and 12th, all clones matching peak 10th (clone number: 4, 52, 79) presented two substitutions at *E. coli* positions 337 (G instead A) and 433 (A instead G) with respect to all other SAR11 sequences. Among *Gammaproteobacteria* sequences, a high variability was found regarding the V3 region, only

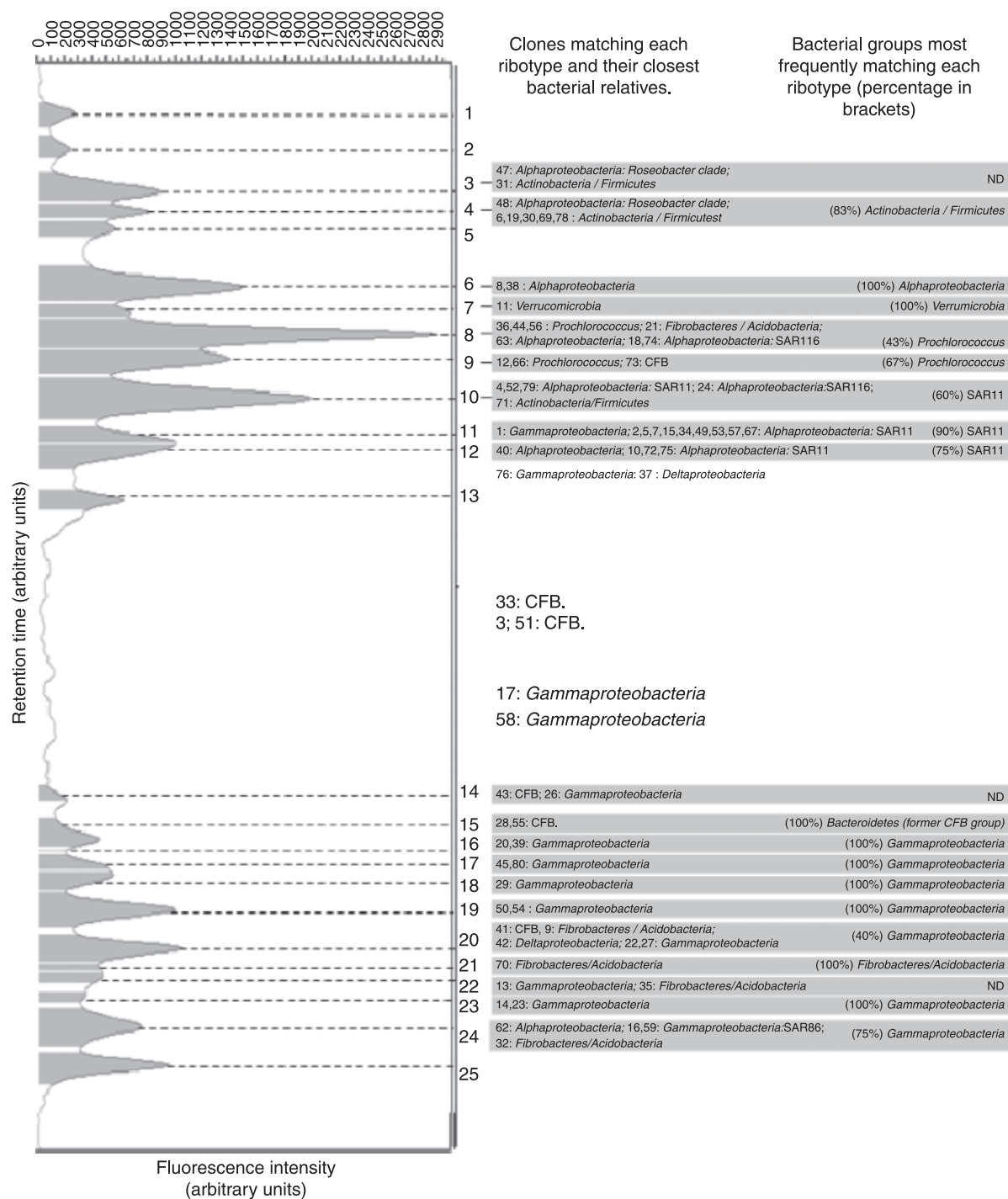


Fig. 5. CE-SSCP bacterial community peaks assignment by clone library-derived profiles, using the GeneScan-400 Rox internal standard as a reference. For each CE-SSCP community peak (on the left-hand side), its matching clones (clone number and phylogenetic affiliation; middle-side) as well as the percentage of the most frequently matching clone pilyotypes per peak (right-hand side) are indicated. ND, nondetermined peak identity.

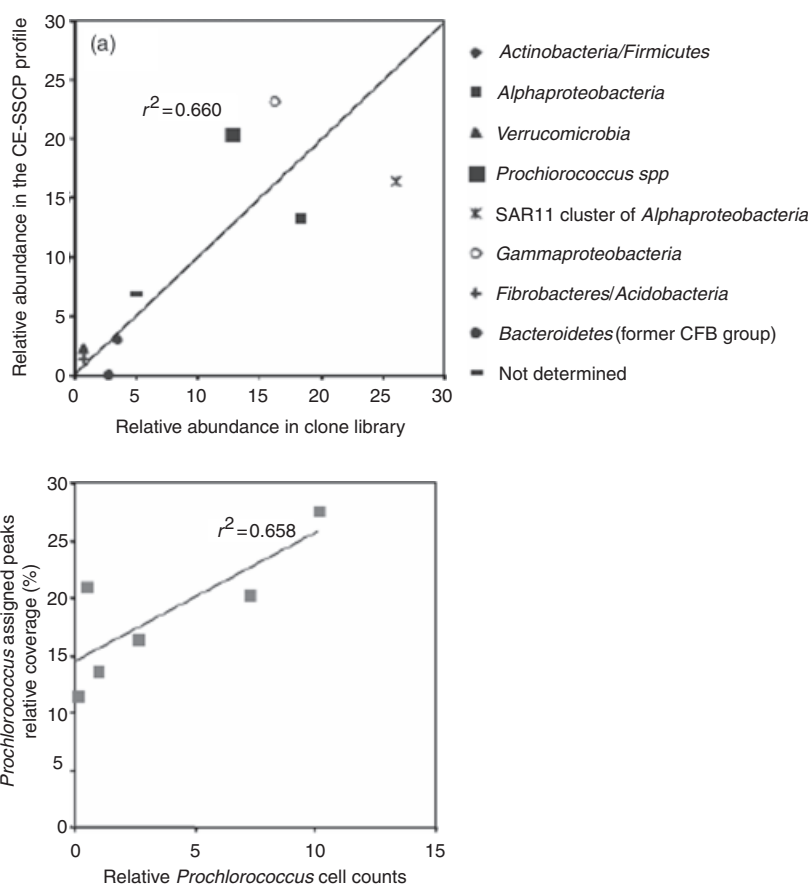


Fig. 6. (a) Spearman's rank pairwise correlation among the relative surface of CE-SSCP ribotypes and the relative importance of the corresponding matching clones on the clone library. (b) Spearman's rank pairwise correlation among relative surface of peaks assigned to *Prochlorococcus* in the total CE-SSCP profile area and the ratio of *Prochlorococcus* cells to the total abundance at the DCM and 20 m below the DCM at stations MOLA, S1 and S2.

clones matching the 12th peak (clone numbers: 12 and 23) specifically shared a consensus sequence (from *E. coli*: 440 to 462 positions). Among *Prochlorococcus* sequences matching the 8th and 9th peaks, there were no shared differences. Therefore, these differences among clones belonging to the same group that matched different peaks were not found to be systematic.

To test the relevance of the comparison between both CE-SSCP fingerprinting and clone library techniques, the relative area of all SSCP peaks assigned to a single phylotype was compared with its relative abundance in the clone library (Fig. 6a). A significantly positive correlation was found ($r^2 = 0.66$, $P < 0.01$), although differences were observed among phylogenetic groups. Thus, the relative abundances of *Prochlorococcus* and *Gammaproteobacteria* were higher in the CE-SSCP fingerprints than in the clone library, while the opposite was found for SAR11, other *Alphaproteobacteria* and *Bacteroidetes* (Fig. 6a). In addition, a significant and positive correlation was also found ($r^2 = 0.66$, $P < 0.05$) between *Prochlorococcus* relative abundance derived from the CE SSCP peaks and cells counted using flow cytometry (Fig. 6b). Altogether, even if absolute abundances cannot be extracted from the CE-SSCP fingerprints, a good agreement

was found between the two techniques for estimating changes in the relative abundance of bacterial populations within the total bacterial community.

Spatial distribution of total and active bacterial populations

We applied the CE-SSCP peaks' identification described above to estimate the bacterial dynamics at the rDNA and rRNA levels, along the surveyed transect (Fig. 7). Overall, 74% of the total fingerprints area (range 65–91%) could be assigned to known phylotypes.

In the surface waters of the three studied stations, the most abundant populations in the rDNA-based fingerprints, were SAR11 (average = 31%, ranging from 22% to 36% among stations) and *Gammaproteobacteria* (22%, ranging from 17% to 26%), followed by *Prochlorococcus* (8%, ranging from 4% to 13%). In the rRNA fingerprints *Prochlorococcus* represented an important fraction of the bacterial community (19%, ranging from 10% to 25%), whereas SAR11 represented only 16% (range 13% to 20%), other *Alphaproteobacteria* (not detected on rDNA fingerprints) accounted for 9% (range 7–12%) and

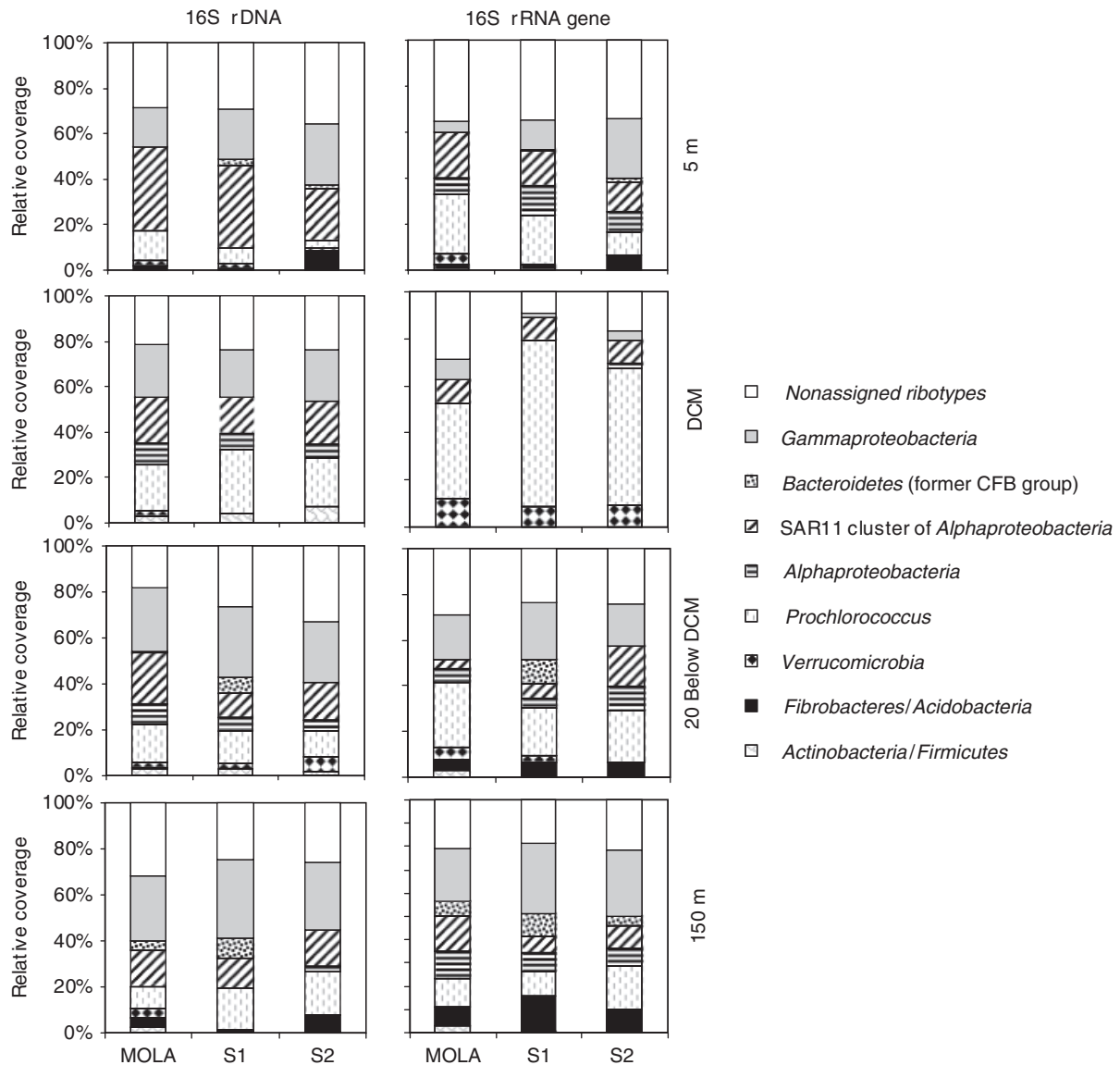


Fig. 7. Spatial variation of bacterial phylotypes' relative coverage on 16S rDNA- (left) and 16S rRNA-based (right) CE-SSCP profiles.

Gammaproteobacteria represented 14% (range 4–26%) of the total fingerprinting area.

The averaged rRNA:rDNA ratio among stations for SAR11 (mean = 0.52, range 0.41–0.58) and *Gammaproteobacteria* (mean = 0.59, range 0.24–0.96) indicated that they were not among the most active populations (Table 1). Conversely, *Prochlorococcus* reached an averaged rRNA:rDNA ratio of 2.59 (range 1.93–3.32).

At the DCM, SAR11 (18%, range 16–20%), *Gammaproteobacteria* (22%, range 20–23%) and *Prochlorococcus* (23%, range 20–27%) were the most abundant groups on 16S rDNA-based fingerprints in the three stations. However, *Prochlorococcus* (56%, range 40–70%) was the most important group on 16S rRNA gene-based fingerprints, represent-

ing *Verrucomicrobia*, SAR11 and *Gammaproteobacteria*, respectively, 10% (range 9–12%), 10% (range 9–10%) and 5% (range 2–9%). *Prochlorococcus* presented an average rRNA:rDNA ratio of 2.4 (range from 2.0 to 2.77), whereas SAR11 (0.55, range 0.49–0.60) and *Gammaproteobacteria* (0.21, range 0.09–0.37) showed much lower ratios. *Verrucomicrobia* phylum was only found among rDNA at MOLA station where its activity ratio was 2.05 (Table 1).

Below the DCM and at 150 m depth, *Gammaproteobacteria* was more abundant both at the rDNA (29%, ranging from 27% to 34%) and at the rRNA level (24%, ranging from 18% to 30%). SAR11 and other *Alphaproteobacteria* were also abundant at the rDNA (19%, ranging from 13% to 31%) and rRNA levels (17%, range 9–27%). Overall,

Table 1. Ratios between relative abundance in the rRNA- and rDNA-based CE-SSCP fingerprints for the main identified phylotypes, at all depths sampled (5 m, DCM depth, 20 m below DCM and 150 m) on each station (MOLA, S1 and S2)

Bacterial phylotypes	5 m			DCM			20 m below DCM			150 m		
	MOLA	S1	S2	MOLA	S1	S2	MOLA	S1	S2	MOLA	S1	S2
<i>Actinobacteria/Firmicutes</i>	–	DNA	–	DNA	DNA	DNA	1.07	DNA	DNA	1.27	1.55	DNA
<i>Verrucomicrobia</i>	2.05	DNA	DNA	5.17	RNA	RNA	2.17	1.05	DNA	DNA	DNA	–
<i>Prochlorococcus</i>	1.93	3.32	2.52	2.00	2.57	2.77	1.74	1.50	1.97	1.34	0.58	1.00
<i>Alphaproteobacteria</i>	RNA	RNA	RNA	DNA	DNA	0.33	0.64	0.69	2.16	RNA	RNA	3.16
SAR11	0.55	0.41	0.58	0.49	0.60	0.55	0.18	0.61	1.10	0.95	0.52	0.64
<i>Bacteroidetes</i> (former CFB)	–	0.30	0.98	–	–	–	DNA	1.54	–	1.39	1.13	RNA
<i>Gammaproteobacteria</i>	0.24	0.58	0.96	0.37	0.09	0.17	0.73	0.81	0.68	0.80	0.89	0.96
<i>Fibrobacteres/Acidobacteria</i>	1.47	RNA	0.77	–	–	–	5.48	RNA	RNA	1.85	RNA	1.38

DNA, only founded on 16S rDNA-based fingerprints; RNA, only founded on 16S rRNA-based fingerprints; –, not founded on both 16S rDNA- and 16S rRNA-based fingerprints.

we observed a high similarity between rDNA and rRNA fingerprints below the DCM, and with rRNA : rDNA ratios close to 1.

Despite the limitations related to comigration mentioned above, we consistently observed differences in the behavior of different microdiverse populations. Thus, SAR11-peak 10 represented on average 60% of the phylotype importance along the water column, whereas SAR11-peak 11 was the most important fraction (50%) of the active communities present at 150 m. In turn, the relative abundance of *Prochlorococcus*-peak 8 was higher on the surface and DCM, while *Prochlorococcus*-peak 9 predominated below DCM and had higher rRNA : rDNA ratios (data not shown).

Discussion

CE-SSCP and community ribotype assignation procedure

There is a general agreement that genetic fingerprints are more adequate tools to study the spatial dynamics of bacterial populations than the more time-consuming cloning approaches. Nonetheless, although fingerprinting methods provide a quick overview of populations dynamics, they remain quite limited for phylogenetic identification of bacterial populations. In the present study, we investigated the interest of combining high-resolution CE-SSCP fingerprinting with clone library to study the spatial distribution of phylogenetically identified bacterial populations.

Using this combined approach, a high percentage of both total peaks (80.0%) and total CE-SSCP area (86.7%) in the fingerprints matched identified clones. These results are in agreement with those found using the same approach in a mine drainage ecosystem (Hong *et al.*, 2007) or by combining clone library with automated ribosomal intergenic spacer analysis (ARISA) in a marine environment (Brown *et al.*, 2005).

Comigration of PCR products from different species within the same peak is a common limitation of fingerprinting methods (Kowalchuk *et al.*, 1997; Vallaeys *et al.*, 1997; Piceno *et al.*, 1999; Casamayor *et al.*, 2000). In our study, we checked this constraint in detail by running the CE-SSCP signature of 80 individual clones in parallel to the natural complex assemblage. As shown by the rarefaction curve (Fig. 4b), these clones may cover the most dominant bacterial phylotypes in our ecosystem. About a half (55%) of the CE-SSCP peaks observed in the natural sample were matched by clone-based peaks belonging to different phylotypes. This result indicates that the 204 bp V3 region of the 16S rRNA gene was not well resolved in CE-SSCP analysis, leading to the presence of different sequences at the same position in the fingerprint. In other studies, peaks matching two or more phylogenetically different clones were assigned to a given phylotype either by (1) using group-specific primers (Brown *et al.*, 2005), by (2) assignation to functional categories (Hong *et al.*, 2007) or (3) being simply discarded for interpretation (West *et al.*, 2008). In our study, comigration represented around half of the CE-SSCP peaks and we have proposed to assign these peaks to the most represented phylotypes that migrate within each peak. We found a significant correlation between the area of the peak or peaks assigned to a given phylotype and its relative importance in the clone library (Fig. 6a). This correlation was in agreement with studies using other fingerprinting techniques (Felske *et al.*, 1998; Casamayor *et al.*, 2000). In addition, we found a significant correlation between the relative areas of *Prochlorococcus* assigned CE-SSCP peaks and its relative cell counts by flow cytometry (Fig. 6b) suggesting that *Prochlorococcus* sequences are amplified according to its real abundance in the sample. Even if a correlation could be established between the area of assigned peaks and other approaches, the information provided by peaks intensity cannot be used as an absolute measure of the abundance. Peak intensity should only be used for comparative purposes among different samples.

Spatial changes of total and active bacterial assemblages

Spatial variation of bacterial community structure was found to be low among the studied stations and to be mainly driven vertically (Fig. 3) as it had been shown previously (Lee & Fuhrman, 1991; Acinas *et al.*, 1997; Ghiglione *et al.*, 2007). Our approach allowed us to focus on bacterial populations presenting these vertical variations both on the whole community (i.e. 16S rDNA) and on the active fraction (16S rRNA).

In surface waters, SAR11 and *Gammaproteobacteria* were dominant among the total bacterial populations, representing around 31% and 22% of the total area of 16S rDNA-based CE-SSCP profiles at 5 m depth in the three stations (Fig. 7). These results were consistent with previous data also obtained at surface depth in offshore waters (Acinas *et al.*, 1999). The predominance of SAR11 has been shown for different sites worldwide (Morris *et al.*, 2002), suggesting that this group may play an important ecological role in marine surface waters. Surprisingly, their importance among active communities was lower than expected according to their relative abundance (16% and 14%, respectively, for SAR11 and *Gammaproteobacteria*). In the same way, previous studies had showed low activity on a per cell basis for SAR11 and also for *Gammaproteobacteria* (Alonso-Saez & Gasol, 2007).

On the contrary, *Prochlorococcus* behaved in the opposite way at the surface and DCM. For example, at the DCM this genus represented on average only 23% of the rDNA-based fingerprints while it accounted for 56% (up to 71% at the MOLA station) of the rRNA-based fingerprints (Fig. 7). This result suggests that most of the *Prochlorococcus* cells would be very active in the photic zone, especially those cells belonging to one of the two ecotypes found (peak 9, Fig. 5). Interestingly, the case of the spatial variation in microdiverse populations found for *Prochlorococcus* appears as especially illustrative because it is in agreement with recent literature on this topic (e.g. Scanlan & West, 2002, and references therein). This group was probably partially responsible for the bacterial activity (leucine incorporation) measured on surface and DCM samples, because amino acids uptake reported previously for *Prochlorococcus* represented up to 50% of the total bacterioplankton consumption in certain depths of Atlantic oceanic oligotrophic regions (Zubkov *et al.*, 2004). Because of their high cell surface/volume ratio, unusual low nutritional requirements and mixotrophic metabolism, *Prochlorococcus* present several competitive advantages that could explain their ecological success in oligotrophic environments (Partensky *et al.*, 1999; Zubkov *et al.*, 2004). Altogether, data are in agreement with the high activity ratios we found at surface and DCM waters for *Prochlorococcus*, and suggest that they play a much more

important functional role in the ecosystem than predicted from their relative abundances and expected autotrophic metabolism. Several minority phylotypes comigrated with *Prochlorococcus* on peaks 8 and 9 (Fig. 5). However, the activity of these groups regarding their corresponding assigned peaks (peak 6 for *Alphaproteobacteria*; peak 21 for *Fibrobacteres/Acidobacteria*; and peak 15 for *Bacteroidetes*) was shown to be very low or nonexistent on 16S rRNA gene profiles at the DCM (Fig. 7), supporting the fact that *Prochlorococcus* activity observed based on peaks 8 and 9 at the DCM could be reliably attributable to this group.

Sequencing data obtained at the DCM also showed low relative importance of *Prochlorococcus*, representing only 6% of the total sequences, whereas other groups like *Alpha-* and *Gammaproteobacteria* presented higher relative importance (Fig. 4a). Using several phylogenetic markers, recent metagenomic studies suggested that 16S rDNA operon number variation may induce an overestimation of the real abundance of phylotypes like *Gammaproteobacteria* and an underestimation of phylotypes like *Cyanobacteria* (*Prochlorococcus*) (Venter *et al.*, 2004). Most of these metagenomic studies have only explored surface waters without taking into account the vertical variation of bacterial community structure. In the sole metagenomic study performed at the DCM layer to date, *Prochlorococcus* presented the highest relative importance with respect to other phylotypes (De-Long *et al.*, 2006), which is consistent with our results. Diversity assessment based on rDNA is widely used and it remains as the accepted standard for uncultured microorganisms (Venter *et al.*, 2004), but further metagenomic data may be needed to confirm these observations.

Only a few studies have simultaneously carried out analysis of population dynamics both at the rDNA and at the rRNA level (Moeseneder *et al.*, 2001, 2005; Troussellier *et al.*, 2002; Winter *et al.*, 2004). This approach allows the comparison of total vs. metabolically active bacterial community structures. We found differences between these two fractions that were in agreement with previously reported results (Moeseneder *et al.*, 2001) and we could identify the main bacterial populations responsible for these divergences. Differences were related to both relative abundances and the presence/absence in one or the other fraction, and most of them were associated with depths having high BP values, i.e. surface waters and the DCM depth. In the case of the DCM, the rRNA fingerprints showed a consistently lower richness than that obtained from rDNA-based fingerprints (Fig. 3a). Furthermore, most of the peaks found on rDNA fingerprints were not detected on the rRNA level, reflecting populations that did not have detectable activity (Fig. 3b). This may be an indication that only a small fraction of the bacterial community was actively taking up leucine, which is in agreement with previous findings

(Servais *et al.*, 2003). Thus, in the photic zone of the oligotrophic NW Mediterranean Sea there is an important heterogeneity of physiological states among natural populations that can be addressed by a combined 16S rDNA/16S rRNA gene approach.

In conclusion, we have shown that the combined study of both 16S rDNA- and 16S rRNA-based approach is very helpful and complementary for the interpretation of changes in the bacterioplankton community structure. We found that the high relative abundance of SAR11 and *Gammaproteobacteria* in the photic zone of oligotrophic sea waters cannot be always related to high relative contribution within the active bacterial fraction. Our results suggest that, at least in this area and at the time of sampling, other groups such as *Prochlorococcus* sp. would play a more important role in the food web than expected. This stresses the need for detailed long-term monitoring at the MOLA station and other microbial observatories coupled to additional environmental parameters to follow with higher resolution the population dynamics and specific changes in the physiological status of the bacterial communities inhabiting the NW Mediterranean Sea.

Acknowledgements

We formally thank Captain and Crew of the RV Thethys for their help during sampling, R. Lami and N. West for advice on CE-SSCP, M. Larcher for her proficiency in clone library construction and J. Guarini for assistance with English grammar. The present work was integrated in the BASICS project (Bacterial single-cell approaches to the relationship between diversity and function in the sea). A.R.B. was supported by a Marie Curie Fellowship from the European Commission and E.O.C. by the Program Ramón y Cajal and REN2003-08333 from the Spanish Ministerio de Educación y Ciencia and FEDER.

References

- Acinas S, Rodríguez-Valera R & Pedros-Alio C (1997) Spatial and temporal variation in marine bacterioplankton diversity as shown by RFLP fingerprinting of PCR amplified 16S rDNA. *FEMS Microbiol Ecol* **24**: 27–40.
- Acinas SG, Antón J & Rodríguez-Valera F (1999) Diversity of free-living and attached bacteria in offshore Western Mediterranean waters as depicted by analysis of genes encoding 16S rRNA. *Appl Environ Microbiol* **65**: 514–522.
- Alonso-Saez L & Gasol JM (2007) Seasonal variations in the contributions of different bacterial groups to the uptake of low-molecular-weight compounds in Northwestern Mediterranean coastal waters. *Appl Environ Microbiol* **73**: 3528–3535.
- Azam F, Fenchel T, Field JG, Gray JS, Meyer-Reil LA & Thingstad F (1983) The ecological role of water-column microbes in the sea. *Mar Ecol Prog Ser* **10**: 257–263.
- Brosius J, Dull TJ, Sleeter DD & Noller HF (1981) Gene organization and primary structure of a ribosomal RNA operon from *Escherichia coli*. *J Mol Biol* **148**: 107–127.
- Brown MV, Schwalbach MS, Hewson I & Fuhrman JA (2005) Coupling 16S-ITS rDNA clone libraries and automated ribosomal intergenic spacer analysis to show marine microbial diversity: development and application to a time series. *Environ Microbiol* **7**: 1466–1479.
- Casamayor EO, Schaefer H, Baneras L, Pedros-Alio C & Muyzer G (2000) Identification of and spatio-temporal differences between microbial assemblages from two neighboring Sulfurous Lakes: comparison by microscopy and denaturing gradient gel electrophoresis. *Appl Environ Microbiol* **66**: 499–508.
- Casamayor EO, Mas J & Pedros-Alio C (2001) *In situ* assessment on the physiological state of purple and green sulfur bacteria through the analyses of pigment and 5S rRNA content. *Microb Ecol* **42**: 427–437.
- Cho BC & Azam F (1990) Biogeochemical significance of bacterial in the ocean's euphotic zone. *Mar Ecol Prog Ser* **63**: 253–259.
- Delbès C, Godon JJ & Moletta R (2001) Bacterial and archaeal 16S rDNA and rRNA dynamics during an acetate crisis in an anaerobic digester ecosystem. *FEMS Microbiol Ecol* **35**: 19–26.
- Del Giorgio PA & Bouvier T (2002) Linking the physiologic and phylogenetic successions in free-living bacterial communities along an estuarine salinity gradient. *Limnol Oceanogr* **47**: 471–486.
- DeLong EF, Wickham GS & Pace NR (1989) Phylogenetic stains: ribosomal RNA-based probes for the identification of single cells. *Science* **243**: 1360–1363.
- DeLong EF, Preston CM, Mincer T *et al.* (2006) Community genomics among stratified microbial assemblages in the ocean's interior. *Science* **311**: 496–503.
- Felske A, Akkermans AD & De Vos WM (1998) Quantification of 16S rRNAs in complex bacterial communities by multiple competitive reverse transcription-PCR in temperature gradient gel electrophoresis fingerprints. *Appl Environ Microbiol* **64**: 4581–4587.
- Ghiglione JF, Larcher M & Lebaron P (2005) Spatial and temporal scales of variation in the bacterioplankton community structure in the NW Mediterranean Sea. *Aquat Microb Ecol* **40**: 229–240.
- Ghiglione JF, Mevel G, Pujo-Pay M, Mousseau L, Lebaron P & Goutx M (2007) Diel and seasonal variations in abundance, activity, and community structure of particle-attached and free-living bacteria in NW Mediterranean Sea. *Microb Ecol* **54**: 217–231.
- Hong H, Pruden A & Reardon KF (2007) Comparison of CE-SSCP and DGGE for monitoring a complex microbial community remediating mine drainage. *J Microbiol Methods* **69**: 52–64.
- Joux F, Servais P, Naudin JJ, Lebaron P, Oriol L & Courties C (2005) Distribution of picophytoplankton and

- bacterioplankton along a river plume gradient in the Mediterranean Sea. *Vie et Milieu* **55**: 197–208.
- Kirchman DL (1993) Leucine incorporation as a measure of biomass production by heterotrophic bacteria. *Handbook of Methods in Aquatic Microbial Ecology* (Kemp PE, Sherr BF, Sherr EB & Cole JJ, eds), pp. 509–512. Lewis Publishers, Boca Raton, FL.
- Kowalchuk GA, Gerards S & Woldendorp JW (1997) Detection and characterization of fungal infections of *Ammophila arenaria* (marram grass) roots by denaturing gradient gel electrophoresis of specifically amplified 18S rDNA. *Appl Environ Microbiol* **63**: 858–865.
- Lee DH, Zo YG & Kim SJ (1996) Non radioactive method to study genetic profiles of natural bacterial communities by PCR-single-strand-conformation-polymorphism. *Appl Environ Microbiol* **62**: 3112–3120.
- Lee SH & Fuhrman JA (1991) Spatial and temporal variation of natural bacterioplankton assemblages studied by total genomic DNA cross-hybridization. *Limnol Oceanogr* **36**: 1277–1287.
- Moeseneder MM, Winter C & Herndl GJ (2001) Horizontal and vertical complexity of attached and free-living bacteria of the eastern Mediterranean Sea, determined by 16S rDNA and 16S rRNA fingerprints. *Limnol Oceanogr* **46**: 95–107.
- Moeseneder MM, Arrieta JM & Herndl GJ (2005) A comparison of DNA- and RNA-based clone libraries from the same marine bacterioplankton community. *FEMS Microbiol Ecol* **51**: 341–352.
- Morris RM, Rappe MS, Connon SA, Vergin KL, Siebold WA, Carlson CA & Giovannoni SJ (2002) SAR11 clade dominates ocean surface bacterioplankton communities. *Nature* **420**: 806–810.
- Murray AE, Preston CM, Massana R, Taylor LT, Blakis A, Wu K & DeLong EF (1998) Seasonal and spatial variability of bacterial and archaeal assemblages in the coastal waters near Anvers Island, Antarctica. *Appl Environ Microbiol* **64**: 2585–2595.
- Neveux J & Panouse M (1987) Spectrofluorometric determination of chlorophylls and pheophytins. *Archiv Hydrobiol* **109**: 567–581.
- Partensky F, Hess WR & Vaulot D (1999) *Prochlorococcus*, a marine photosynthetic prokaryote of global significance. *Microbiol Mol Biol Rev* **63**: 106–127.
- Pernthaler J & Amann R (2005) Fate of heterotrophic microbes in pelagic habitats: focus on populations. *Microbiol Mol Biol Rev* **69**: 440–461.
- Piceno YM, Noble PA & Lovell CR (1999) Spatial and temporal assessment of diazotroph assemblage composition in vegetated salt marsh sediments using denaturing gradient gel electrophoresis analysis. *Microb Ecol* **38**: 157–167.
- Poulsen LK, Ballard G & Stahl DA (1993) Use of rRNA fluorescence *in situ* hybridization for measuring the activity of single cells in young and established biofilms. *Appl Environ Microbiol* **59**: 1354–1360.
- Riemann L, Steward GF, Fandino LB, Campbell L, Landry MR & Azam F (1999) Bacterial community composition during two consecutive NE Monsoon periods in the Arabian Sea studied by denaturing gradient gel electrophoresis (DGGE) of rDNA. *Deep-Sea Res II* **46**: 1791–1811.
- Scanlan DJ & West NJ (2002) Molecular ecology of the marine cyanobacterial genera *Prochlorococcus* and *Synechococcus*. *FEMS Microb Ecol* **40**: 1–12.
- Schauer M, Massana R & Pedrós-Alió C (2000) Spatial differences in bacterioplankton composition along the Catalan coast (NW Mediterranean) assessed by molecular fingerprinting. *FEMS Microbiol Ecol* **33**: 51–59.
- Schloss PD & Handelsman J (2005) Introducing DOTUR, a computer program for defining operational taxonomic units and estimating species richness. *Appl Environ Microbiol* **71**: 1501–1506.
- Servais P, Casamayor EO, Courties C, Catala P, Parthuisot N & Lebaron P (2003) Activity and diversity of high and low nucleic acid content bacterial cells. *Aquat Microb Ecol* **33**: 41–51.
- Sherr BF, Del Giorgio PA & Sherr EB (1999) Estimating the abundance and single-cell characteristics of respiring bacteria via the redox dye CTC. *Aquat Microb Ecol* **18**: 117–131.
- Smith DC & Azam F (1992) A simple, economical method for measuring bacterial protein synthesis rates in seawater using 3H-leucine. *Mar Microb Food Webs* **6**: 107–114.
- Thompson JD, Gibson TJ, Plewniak F, Jeanmougin F & Higgins DG (1997) The CLUSTAL_X windows interface: flexible strategies for multiple sequence alignment aided by quality analysis tools. *Nucleic Acids Res* **25**: 4876–4882.
- Troussellier M, Schäfer H, Batailler N, Bernard L, Courties C, Lebaron P, Muyzer G, Servais P & Vives-Rego J (2002) Bacterial activity and genetic richness along an estuarine gradient (Rhône River plums, France). *Aquat Microb Ecol* **28**: 13–24.
- Vallaëys T, Topp E, Muyzer G, Macheret V, Laguerre G, Rigaud A & Soulas G (1997) Evaluation of denaturing gradient gel electrophoresis in the detection of 16S rDNA sequence variation in rhizobia and methanotrophs. *FEMS Microbiol Ecol* **24**: 279–285.
- Venter JC, Remington K, Heidelberg JF et al. (2004) Environmental genome shotgun sequencing of the Sargasso Sea. *Science* **304**: 66–74.
- West NJ, Obernosterer I, Zemb O & Lebaron P (2008) Major differences of bacterial diversity and activity inside and outside of a natural iron-fertilized phytoplankton bloom in the Southern Ocean. *Environ Microbiol* **10**: 738–756.
- Winter C, Herndl G & Weinbauer MG (2004) Diel cycles in viral infection of bacterioplankton in the North Sea. *Aquat Microb Ecol* **35**: 207–216.
- Zemb O, Haegeman B, Delgenes JP, Lebaron P & Godon JJ (2007) Safum: statistical analysis of SSCP fingerprints using PCA projections, dendrograms and diversity estimators. *Mol Ecol Notes* **7**: 767–770.
- Zubkov MV, Tarran GA, Bernhard M & Fuchs BM (2004) Depth related amino acid uptake by *Prochlorococcus* cyanobacteria in the Southern Atlantic tropical gyre. *FEMS Microbiol Ecol* **50**: 153–161.